Seasonal drought events in tropical East Asia over the last 60,000 y

Jianping Zhang[a,b,1,2], Houyuan Lu[a,b,c,1,2], Jiwei Jia[a,3,4], Caiming Shen[d], Shuyun Wang[a,3,5], Guoqiang Chu[a], Luo Wang[a], Anning Cui[a,c], Jiaqi Liu[a], Naiqin Wu[a], and Fengjiang Li (李丰江)[a]

[a]Key Laboratory of Cenozoic Geology and Environment, Institute of Geology and Geophysics, Chinese Academy of Sciences, 100029, Beijing, China; [b]Center for Excellence in Tibetan Plateau Earth Sciences, Chinese Academy of Sciences, 100101, Beijing, China; [c]College of Earth and Planetary Sciences, University of Chinese Academy of Sciences, 101408, Beijing, China; and [d]Yunnan Key Laboratory of Plateau Geographical Processes and Environmental Changes, College of Tourism and Geographical Sciences, Yunnan Normal University, 650500, Kunming, China

Edited by Dolores R. Piperno, Smithsonian Institution, Washington, DC, and approved October 8, 2020 (received for review July 2, 2020)

The cause of seasonal hydrologic changes in tropical East Asia during interstadial/stadial oscillations of the last glaciation remains controversial. Here, we show seven seasonal drought events that occurred during the relatively warm interstadials by phytolith and pollen records. These events are significantly manifested as high percentages of bilobate phytoliths and are consistent with the large zonal sea-surface temperature (SST) gradient from the western to eastern tropical Pacific, suggesting that the reduction in seasonal precipitation could be interpreted by westward shifts of the western Pacific subtropical high triggered by changes of zonal SST gradient over the tropical Pacific and Hadley circulation in the Northern Hemisphere. Our findings highlight that both zonal and meridional ocean–atmosphere circulations, rather than solely the Intertropical Convergence Zone or El Niño-Southern Oscillation, controlled the hydrologic changes in tropical East Asia during the last glaciation.

phytolith | pollen | interstadial/stadial | tropical SST gradient | Walker and Hadley circulation

The tropics are home to regions of central importance to global hydrologic cycles. As an important hydrological parameter, seasonal precipitation underwent profound changes in the tropical oceans and their adjacent continents on different timescales during the last glaciation (1). However, the features and mechanisms that caused seasonal precipitation changes during interstadial/stadial oscillations of the last glacial–interglacial cycle in tropical regions remain controversial (2). Two contrasting hypotheses were proposed to explain these changes. Both of these hypotheses involve interactions between the meridional Hadley and zonal Walker circulations as well as changes in sea-surface temperature (SST) (3).

The first hypothesis invokes tropical SST changes in response to a slowdown of the Atlantic Meridional Overturning Circulation (AMOC) triggered by large iceberg discharges in the North Atlantic during the stadials (4, 5) and the resulting shift of the intertropical convergence zone (ITCZ). This AMOC-forced southward movement of the ITCZ caused antiphase changes in seasonal rainfall between north and south of the equator in the tropical Pacific and its adjacent continents on the millennium scale (6–9). The second hypothesis attributes the changes in the tropical atmosphere–ocean dynamics stimulated by tropical SST changes (e.g., El Niño-Southern Oscillation, ENSO) (10, 11) as the cause of seasonal heavy/light rainfall in the eastern/western tropical Pacific during the Heinrich stadials (12).

However, most of the evidence supporting these two hypotheses comes from the Atlantic (13) and the tropical Pacific (1, 12, 14). Limited evidence is from tropical continents, and particularly little evidence is available from terrestrial tropical East Asia, where the mechanisms responsible for seasonal precipitation changes are still under debate. Although the oxygen isotopes of stalagmites on land have been viewed as one of the most robust East Asian summer monsoon records, the interpretation of speleothem $\delta^{18}O$ in China remains controversial (15–17). Therefore, to demonstrate these hypotheses, both unique research sites, which could simultaneously receive continental and tropical ocean signals, and unambiguous proxies, which could reflect annual and seasonal precipitation, are urgently needed.

The core studied in this paper is located at Huguangyan Maar Lake (HML) in Guangdong, southern coast of China (110°17′ E, 21°9′ N, 23 m above sea level) (Fig. 1). This region is closely influenced by Hadley circulation (HC) over the continent and Walker circulation (WC) over the tropical Pacific (18, 19), as well as the related changes in the western Pacific subtropical high (WPSH) (19, 20). Here, we present two sets of proxy datasets. One proxy is the phytolith record, a reliable indicator for the evaluation of seasonal–annual Poaceae in ecosystems (21, 22); and Poaceae taxa are more sensitive than arboreal taxa in revealing seasonal hydrological changes (21, 22). The other proxy is the pollen record, which is an indicator of annual precipitation and reflects the general paleoclimate features at low latitudes in East Asia (23–29). Therefore, based on the two contrasting proxies, the successive 60,000-y phytolith and pollen sequences in

Significance

The characters and mechanisms of seasonal precipitation changes during the last glaciation in tropical East Asia are enduring and important issues of debate for researchers from many disciplines. Sensitive indicators for annual/seasonal hydrological changes are keys to understanding the issues. Here, we use successive phytolith and pollen records to reconstruct the changes of precipitation in the catchment of the Huguangyan Maar Lake, an important site at northern tropical East Asia that could simultaneously receive climate signals from higher-latitude continent and tropical ocean. We then identify seven seasonal drought events during interstadials. The results indicate that both zonal and meridional circulations control seasonal hydrologic changes, which is of great significance to understand tropical atmospheric–ocean interactions under global changes.

Author contributions: H.L. designed research; J.Z., H.L., J.J., S.W., G.C., L.W., A.C., J.L., N.W., and F.L. performed research; J.Z. and H.L. contributed new reagents/analytic tools; J.Z., H.L., and C.S. analyzed data; and J.Z., H.L., and C.S. wrote the paper.

The authors declare no competing interest.

This article is a PNAS Direct Submission.

[1]J.Z. and H.L. contributed equally to this work.

[2]To whom correspondence may be addressed. Email: jpzhang@mail.iggcas.ac.cn or houyuanlu@mail.iggcas.ac.cn.

[3]J.J. and S.W. contributed equally to this work.

[4]Present address: Mechanical and Electrical Business Department, Zhengzhou Zhongke Electromechanical Equipment Co., Ltd., 450016, Zhengzhou, China.

[5]Present address: Quality Management Department, BGI Engineering Consultants Ltd., 100038, Beijing, China.

This article contains supporting information online at https://www.pnas.org/lookup/suppl/doi:10.1073/pnas.2013802117/-/DCSupplemental.

First published November 23, 2020.

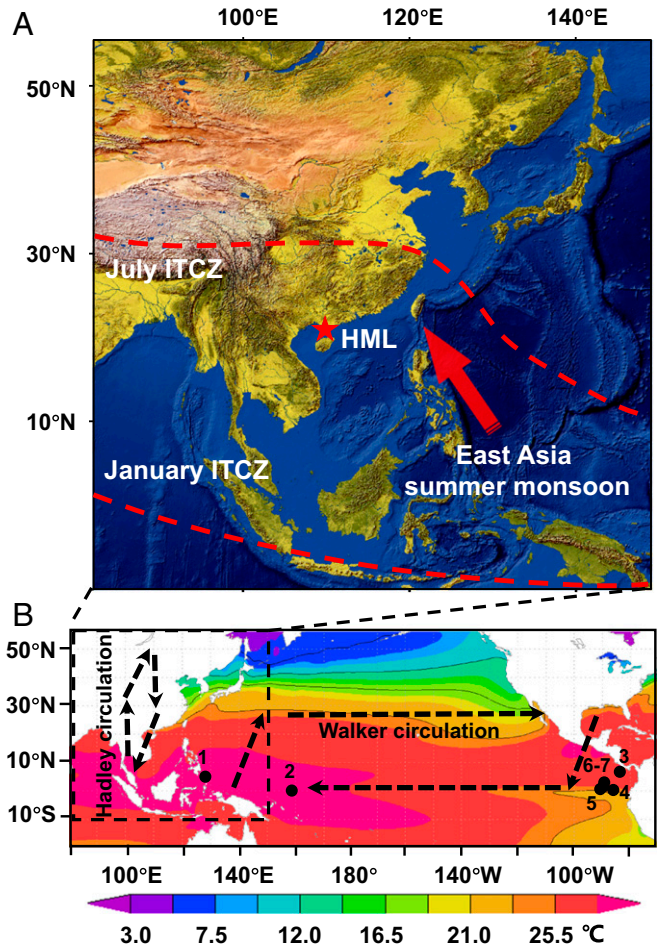

Fig. 1. Geographical and climatological settings of study site and region. (*A*) Topographic map from ENVI 5.1 showing the location of study site (red star, Huguangyan Maar Lake, HML) in south China and seasonal positions of ITCZ (30). (*B*) Schematic map showing the settings of atmospheric circulations and SSTs in the tropical Pacific. Black solid circles indicate cores mentioned in this paper: 1 = MD98-2181, 2 = ODP806B, 3 = MD02-2529, 4 = ME0005A-24JC, 5 = ODP846, 6 = TR163-22, and 7 = TR163-19. Colors are annual mean SSTs from the period 1981–2010 obtained from https://psl.noaa.gov.

this study could substantially reveal the mechanism of regional seasonal precipitation changes during stadials/interstadials since the last glacial period in northern tropical East Asia.

Results

Paleovegetation Dynamics in the Last 60 ka. A total of 113 families and genera of pollen and 23 phytolith morphotypes (28, 31) were identified from a 24.20-m-depth core in HML covering the past 60 ka based on 22 AMS (accelerator mass spectrometry) ^{14}C dates (*SI Appendix*, Figs. S1 and S2 and Table S1). In total, 233 samples at a 10-cm interval clearly revealed three stages (S1, S2, S3) of paleovegetation evolution: the vegetation changed from southern subtropical evergreen and deciduous broad-leaved mixed forest during 60–40 ka BP (ka BP = 1,000 calibrated years Before Present), which was featured by high contents of both tropical–subtropical arboreal taxa and deciduous arboreal taxa (S1), to deciduous broad-leaved forest dominated by ∼20% of *Quercus* (Deciduous) mixed with herb taxa dominated by ∼45% of Poaceae and ∼10% of *Artemisia* during 40–12 ka BP (S2). Since 12 ka BP, the vegetation has changed to tropical seasonal rainforest, which resembled modern vegetation types, characterized by the high contents of arboreal Palmae and Moraceae as well as herbaceous Poaceae taxa, e.g., Bambusoideae and Eragrostoideae (S3) (Fig. 2 and *SI Appendix*, Figs. S3–S5).

The most striking features of the HML phytolith record are seven sharp increases in bilobates (including former dumbbell and cross-types), which are defined as events when the percentage of bilobates sharply increases to more than ∼15%. We named these events as B1 (bilobate event 1) (16.4%, peak value of bilobate percentage, the same below), B2 (33.9%), B3 (12.5%), B4 (30.0%), B5 (19.1%), B6 (19.2%), and B7 (20.4%) (Fig. 2). Furthermore, the seven bilobate events occurred at 10.1–10.8, 14.3–14.9, 26.2–26.4, 32.1–32.9, 44.0–46.7, 48.4–48.9, and 59.2–60.0 ka BP, corresponding to the time of the largest SST gradient during the interstadials (*SI Appendix*, Table S2, Fig. S6). To clarify the paleoclimatic significance represented by the prosperity of bilobates, it is necessary to analyze its modern process in detail.

Climatic Significance of Bilobates in the Topsoil of China. We analyzed 240 topsoil samples collected from eight major vegetation regions across China, from forest to steppe to desert, along a precipitation gradient (32). Fig. 3 reveals that the topsoil bilobate content presents a rise–fall pattern with increasing mean annual precipitation (MAP). The content of bilobate first increases rapidly with increasing MAP and then decreases sharply when the MAP reaches 1,250 mm. The highest content of bilobates occurs at MAPs between 500 and 1,250 mm; in particular almost all topsoil samples with bilobate contents higher than 10% fall in the regions where the MAP is less than 1,250 mm (Fig. 3).

Discussion and Conclusions

Phytolith and Pollen Records Reveal Seven Drought Events during the Last 60 ka. Our pollen record together with other pollen records in tropical and subtropical evergreen forest zones (33, 34) (*SI Appendix*, Fig. S7) revealed hydrological changes and thus Asian monsoon changes that followed the Northern Hemisphere high-latitude (65°N) summer (integrated over June, July, and August) insolation at the glacial–interglacial scale (Fig. 4), whereas our phytolith record, sensitive proxy of seasonal climate changes, revealed seven seasonal drought events under interstadial/stadial oscillations during the relatively arid glacial conditions of the last 60 ka in northern tropical East Asia.

Bilobates are a typical type of phytolith derived mainly from Panicoideae of C_4 grasses (35). Topsoil samples with bilobate contents over 15% only occur in the regions where the MAP ranges between 750 and 1,250 mm (Fig. 3), which is consistent with the result of a previous study that the annual precipitation in the area dominated by C_4 plants was limited in a range of 500–1,200 mm (36). Although temperature controls the growth of C_4 plants, they will dominate the landscape only when precipitation declines as temperature increases, even in regions where the temperature is high enough for the growth of C_4 plants in tropical regions (36). Furthermore, as spring and summer are the growing seasons for C_3 and C_4 plants (37), the decrease in spring rainfall and the subsequent drier conditions in summer would suppress C_3 plants and contribute to the expansion of C_4 plants in tropical regions. Therefore, the sharp increases in bilobates beyond 15% at the HML, where the MAP is over 1,600 mm at present (28), represent the reduction in seasonal rainfall, suggesting that the increase in the bilobate proportion is mainly due to the expansion of Panicoideae. Both of phytolith accumulation rate and abundance for the bilobate show significant increases during seven drought events, indicating that this expansion is largely contributed by favorable climate conditions and the decline of lake level resulting in more living space of Panicoideae (*SI Appendix*, Fig. S8).

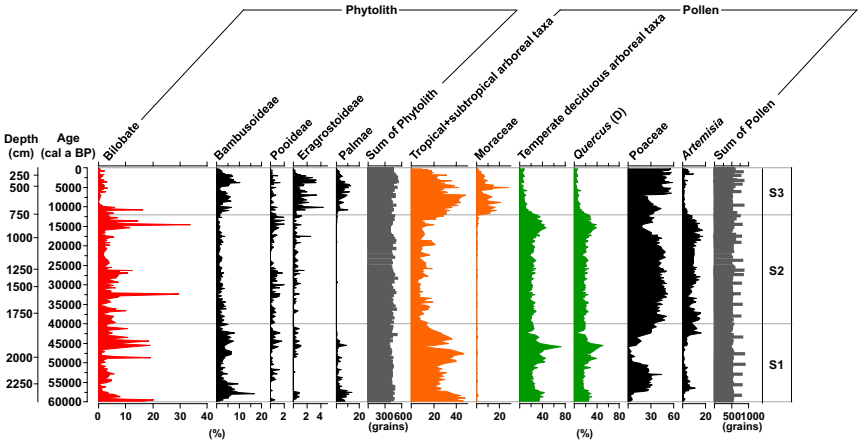

Fig. 2. Phytolith and pollen diagram of HML core B. Only selected taxa are shown, cal a BP (calibrated year Before Present).

Zonal SST Gradients Control the Hydrological Variability According to Walker and Hadley Circulation Changes. The seven events preferentially occurred during periods with large zonal SST gradients (ΔSST) reconstructed from the western (12, 38) to eastern (38–42) tropical Pacific (*SI Appendix*, Fig. S6), and corresponded to Dansgaard–Oeschger events (D/O events) 1, 3, 5, 12, 13, and 17 at high latitudes as compared with the NGRIP (North Greenland Ice Core Project) $\delta^{18}O$ record over the last 60 ka (43, 44) (Fig. 4, *SI Appendix*, Table S2). The evidence indicates that the hydrological fluctuations in the study region are principally influenced by the tropical Pacific ΔSST. We propose that the prolonged effect of ΔSST fluctuations on precipitation is achieved through the westward-shifted WPSH via Walker and Hadley circulation changes over the western Pacific during the interstadials of the last glaciation.

Warm SSTs in the western tropical Pacific reduce convections in the eastern Pacific, resulting in an anticyclonic gyre in the North Pacific, which is favorable to the westward extension of the WPSH (19). Meanwhile, increased western tropical Pacific SST enhances the East Asia Hadley circulation (EAHC) (51, 52), and the increased EAHC would subsequently enhance its descending branches located around 30°N and further reinforce the WPSH (53). The flows returning to low latitudes in the lower troposphere (northeastern wind) would further suppress the East Asian summer monsoon and delay northward migration of the WPSH, thus finally decreasing the water vapor from the ocean and rainfall (18) (Fig. 4*F*). Modern climatological record shows that the spring and summer precipitation in HML in the years when the WPSH moved westward was significantly lower than that in the years when the WPSH moved eastward (Fig. 4*G*), supporting our hypothesis.

Although the AMOC-forced ITCZ movement is the prevailing explanation for the tropical hydrological records (9, 54), a single ITCZ mechanism is difficult to reconcile with the dry interstadial conditions inferred from our HML records. Based on the ITCZ mechanism, drier conditions in tropical East Asia should occur at stadials when the ITCZ moves southward (55). We speculate that the contradiction is because the shift of the mean ITCZ position is small, which has been proven by model and observation research (56).

Combined with other evidence (25, 27, 57), our pollen and phytolith records indicated that the vegetation was dominated by subtropical evergreen forests with deciduous arboreal taxa during cold glacial periods and that the vegetation was eventually transformed into tropical monsoon rainforests until the Holocene. The crown-closed rainforest under the warm and humid climate would possibly suppress the growth of C_4 plants, whereas the dry glacial period and open environment would make the growth of C_4 plants more sensitive to hydrological changes. Therefore, the phytolith content during the Holocene did not follow the ΔSST variation. The increased sea level (Fig. 4*B*) and the consequent shrunken continent, which drove the northward migration of the Asian monsoon rain belt (58) during deglaciation, might make a great contribution to the transformation of vegetation.

We provide well-dated successive terrestrial phytolith and pollen records, revealing that seasonal hydrological changes in tropical East Asia were greatly controlled by the SST gradient over the western to eastern tropical Pacific during the last glaciation. The region experienced at least seven dry events, which promoted the growth of Panicoideae during relatively warm interstadial periods. An explanation of this phenomenon is focused on the variations in the WPSH west-edge position via changes in the WC and EAHC linked with the zonal SST gradient over the tropical Pacific. Based on substantial evidence, it is suggested

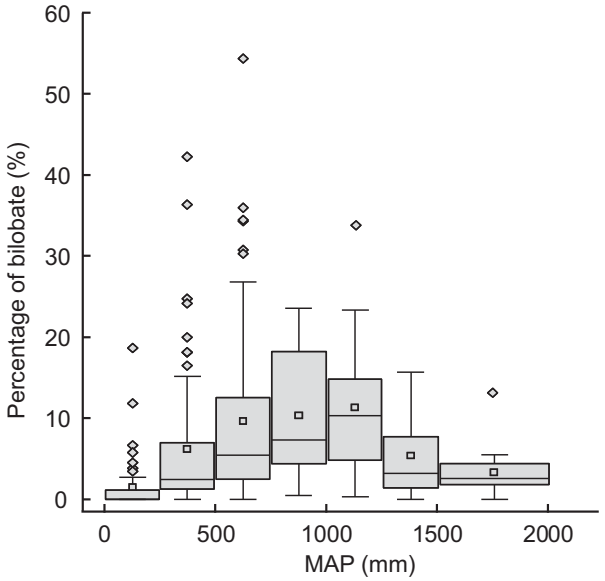

Fig. 3. Boxplot of topsoil bilobate percentage distribution with the mean annual precipitation (MAP) for 240 soil samples across China. Each boxplot indicates the topsoil bilobate percentage in every 250-mm MAP interval, the square in the box indicates the mean value, and the diamond refers to outliers.

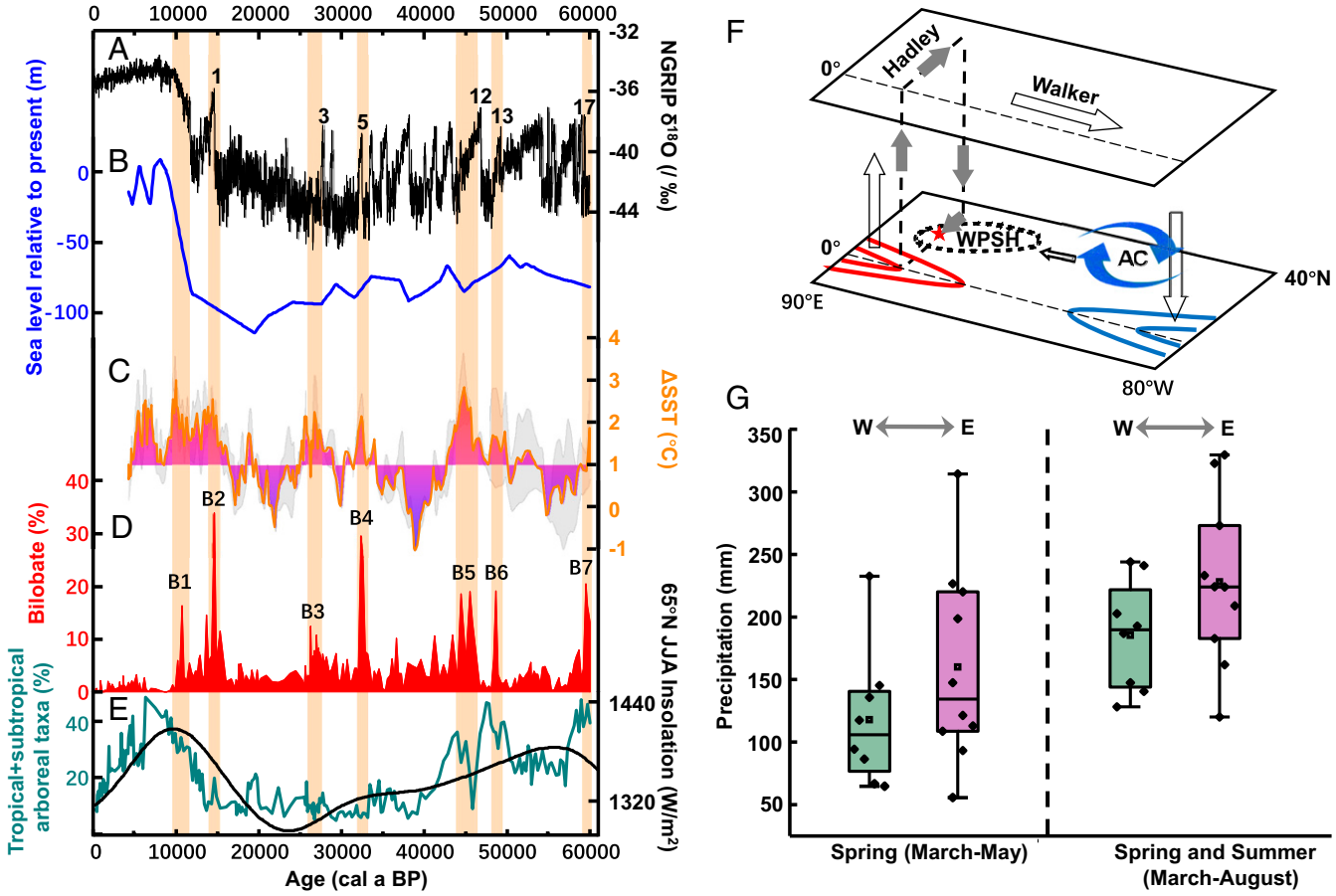

Fig. 4. Comparison of multiproxy data from the HML core with regional and global climatic records over the past 60 ka, schematic diagram showing circulation anomalies, and regional rainfalls associated with these circulation anomalies. (*A*) $\delta^{18}O$ record from NGRIP (on a GICC05 timescale) (45–48), numbers indicate D/O events; (*B*) global sea-level changes (49); (*C*) ΔSST of the western (12, 38) and eastern (39) tropical Pacific; gray indicates the SD of ΔSST; (*D*) percentage of bilobates from HML, B1-B7 indicate seven bilobate events; (*E*) pollen percentage of tropical and subtropical arboreal taxa from HML together with 65°N summer insolation (June, July, and August, JJA) (black line); (*F*) schematic diagram showing circulation anomalies with positive and negative heating (red and blue curves) in the western and eastern tropical Pacific, respectively; "AC" indicates anticyclonic circulation; (*G*) modern precipitation recorded by the Zhanjiang Meteorological Station in the years when the WPSH moves to the westernmost (green bar, W) and easternmost (pink bar, E) locations during spring and spring–summer. We defined the center of the WPSH by the average 588 dagpm (10^1geopotential meter) at 500 hPa; the westward shift years are 1980, 1983, 1988, 1991, 1996, 1998, 2003, and 2010, and the eastward shift years are 1984, 1985, 1986, 1992, 1994, 1997, 1999, 2000, 2002, and 2004 (50). The meteorological data are from the China Meteorological Data Service Center (http://data.cma.cn).

that both zonal and meridional ocean–atmosphere circulations, rather than solely the ITCZ (54) or ENSO (12), play fundamental roles in influencing tropical East Asia hydrology and further shed light on the mechanism of local vegetation responses under global changes at different timescales.

Materials and Methods

The 24.28-m length of HML core B is retrieved from a water depth of 13 m using an Usinger piston corer. The sediments are macroscopically homogeneous, greenish black, highly organic gyttja with occasional indistinct layers (24, 59) (*SI Appendix*, Fig. S1).

A total of 23 phytolith morphotypes were identified from 233 samples of HML core B, which includes a previously published 10,000-y-long phytolith sequence (10–20 ka) (60), according to the classification system of Lu et al. (32), which was modified from three other classifications (61–63) (*SI Appendix*, Fig. S4). Phytolith abundance was expressed as the percentages of all phytoliths counted (*SI Appendix*, Fig. S5). For the identification of bilobates, the article published by Lu et al. (35) was used as a reference. The bilobate types from our core samples could be identified as Panicoideae according to the morphological characteristics of lobes and shanks (35). Parts of the pollen sequence of core B, dating from 13 to 40 ka, 8–18.5 m, have already been published (28). In this study, we provide the whole pollen sequence, which includes a total of 113 families and genera of pollen taxa. Pollen identification was aided with two references (64, 65). Pollen percentages were calculated using the sum of pollen and spores. C2 (Version 1.7.7) software was applied to the phytolith and pollen percentage data to extract the changes in vegetation (66).

Constructions of the relation between modern climate and phytolith morphtypes are based on the data of 240 soil samples from 8 major vegetation regions across China and modern climatic data from a database consisting of 722 meteorological stations (32).

The chronology of HML core B was reconstructed by linear interpolation of 22 AMS radiocarbon age control points (*SI Appendix*, Fig. S2 and Table S1), which have already been published (24, 60), including 16 ages of plant remains and 6 ages of bulk samples. All ^{14}C ages were converted to calendar ages using the IntCal 13 curve (67). The sediment section of HML extends back to 60 ka BP and is characterized by sedimentation rates ranging from ~40 cm ka^{-1} prior to the Holocene to ~0.110 cm ka^{-1} during the past 10,000 y.

Data Availability. All study data are included in the article and *SI Appendix*.

ACKNOWLEDGMENTS. We thank two anonymous reviewers for several insightful comments that significantly improved the paper. We thank Drs. Jörg F.W. Negendank, Xiangjun Lu, Wenyuan Wang, Jens Mingram, and Georg Schettler for field work. This study was supported by the Strategic Priority Research Program of Chinese Academy of Sciences, Grant XDB26000000, the National Natural Science Foundation of China, Grants 41830322, 41372191, and 41888101, Yunnan Project for the Introduction of Advanced Talents (Project 2013HA024), and Youth Innovation Promotion Association of the Chinese Academy of Sciences.

1. Z. F. Xiong *et al*., Rapid precipitation changes in the tropical West Pacific linked to North Atlantic climate forcing during the last deglaciation. *Quat. Sci. Rev.* **197**, 288–306 (2018).
2. J. E. Tierney *et al*., Northern hemisphere controls on tropical southeast African climate during the past 60,000 years. *Science* **322**, 252–255 (2008).
3. J. C. H. Chiang, The tropics in paleoclimate. *Annu. Rev. Earth Planet. Sci.* **37**, 263–297 (2009).
4. W. S. Broecker, Does the trigger for abrupt climate change reside in the ocean or in the atmosphere? *Science* **300**, 1519–1522 (2003).
5. S. Rahmstorf, Ocean circulation and climate during the past 120,000 years. *Nature* **419**, 207–214 (2002).
6. D. S. G. Thomas, R. Bailey, P. A. Shaw, J. A. Durcan, J. S. Singarayer, Late quaternary highstands at Lake Chilwa, Malawi: Frequency, timing and possible forcing mechanisms in the last 44 ka. *Quat. Sci. Rev.* **28**, 526–539 (2009).
7. G. H. Denton *et al*., The last glacial termination. *Science* **328**, 1652–1656 (2010).
8. R. Zhang, T. L. Delworth, Simulated tropical response to a substantial weakening of the Atlantic thermohaline circulation. *J. Clim.* **18**, 1853–1860 (2005).
9. J. C. Stager, D. B. Ryves, B. M. Chase, F. S. R. Pausata, Catastrophic drought in the Afro-Asian monsoon region during Heinrich event 1. *Science* **331**, 1299–1302 (2011).
10. R. G. Wu, B. Wang, A contrast of the east Asian summer monsoon-ENSO relationship between 1962-77 and 1978-93. *J. Clim.* **15**, 3266–3279 (2002).
11. H. Yan *et al*., South China Sea hydrological changes and Pacific Walker Circulation variations over the last millennium. *Nat. Commun.* **2**, 293 (2011).
12. L. Stott, C. Poulsen, S. Lund, R. Thunell, Super ENSO and global climate oscillations at millennial time scales. *Science* **297**, 222–226 (2002).
13. L. C. Peterson, G. H. Haug, K. A. Hughen, U. Röhl, Rapid changes in the hydrologic cycle of the tropical Atlantic during the last glacial. *Science* **290**, 1947–1951 (2000).
14. Q. Jia *et al*., Hydrological variability in the western tropical Pacific over the past 700 kyr and its linkage to Northern Hemisphere climatic change. *Palaeogeogr. Palaeoclimatol. Palaeoecol.* **493**, 44–54 (2018).
15. T. Caley, D. M. Roche, H. Renssen, Orbital Asian summer monsoon dynamics revealed using an isotope-enabled global climate model. *Nat. Commun.* **5**, 5371 (2014).
16. M. Tan, Circulation effect: Response of precipitation $\delta^{18}O$ to the ENSO cycle in monsoon regions of China. *Clim. Dyn.* **42**, 1067–1077 (2014).
17. X. L. Yang *et al*., Holocene stalagmite $\delta^{18}O$ records in the east Asian monsoon region and their correlation with those in the Indian monsoon region. *Holocene* **24**, 1657–1664 (2014).
18. G. Zeng, Z. Sun, W.-C. Wang, J. Min, Interdecadal variability of the east Asian summer monsoon and associated atmospheric circulations. *Adv. Atmos. Sci.* **24**, 915–926 (2007).
19. T. Zhou *et al*., Why the western Pacific subtropical high has extended westward since the late 1970s. *J. Clim.* **22**, 2199–2215 (2009).
20. R. H. Huang, F. Y. Sun, Impacts of the tropical western Pacific on the East-Asian summer monsoon. *J. Meteorol. Soc. Jpn.* **70**, 243–256 (1992).
21. D. R. Piperno, *Phytolith: A Comprehensive Guide for Archaeologists and Paleoecologists* (AltaMira Press, New York, 2006), p. 238.
22. C. A. E. Strömberg, Using phytolith assemblages to reconstruct the origin and spread of grass-dominated habitats in the great plains of North America during the late Eocene to early Miocene. *Palaeogeogr. Palaeoclimatol. Palaeoecol.* **207**, 239–275 (2004).
23. Z. Zheng, Z. Q. Lei, A 400,000 year record of vegetational and climatic changes from a volcanic basin, Leizhou Peninsula, southern China. *Palaeogeogr. Palaeoclimatol. Palaeoecol.* **145**, 339–362 (1999).
24. J. Mingram *et al*., The Huguang Maar Lake-a high-resolution record of palaeoenvironmental and palaeoclimatic changes over the last 78,000 years from South China. *Quat. Int.* **122**, 85–107 (2004).
25. H. Lu *et al*., A study of pollen and environment in the Huguangyan Maar Lake since the last glaciation. *Acta Palaeontologica Sin.* **42**, 284–291 (2003).
26. J. B. Xue, W. Zhong, L. C. Xie, I. Unkel, Millennial-scale variability in biomass burning covering the interval similar to 41,000-7050 cal BP in the tropical Leizhou Peninsula (south China). *Palaeogeogr. Palaeoclimatol. Palaeoecol.* **438**, 344–351 (2015).
27. Y. T. Meng, W. M. Wang, J. F. Hu, J. X. Zhang, Y. J. Lai, Vegetation and climate changes over the last 30000 years on the Leizhou Peninsula, southern China, inferred from the pollen record of Huguangyan Maar Lake. *Boreas* **46**, 525–540 (2017).
28. S. Y. Wang *et al*., Palaeovegetation and palaeoclimate in low-latitude southern China during the last glacial maximum. *Quat. Int.* **248**, 79–85 (2012).
29. X. J. Sun, X. Li, A pollen record of the last 37 ka in deep sea core 17940 from the northern slope of the south China Sea. *Mar. Geol.* **156**, 227–244 (1999).
30. X. F. Zheng *et al*., ITCZ and ENSO pacing on east Asian winter monsoon variation during the Holocene: Sedimentological evidence from the Okinawa trough. *J. Geophys. Res. Oceans* **119**, 4410–4429 (2014).
31. S. Wang, "Paleovegetation and paleoenvironment history recorded by pollen assemblages from the Huguangyan Maar Lake, Southern China since the last 80 ka" (Institute of Geology and Geophysics, Chinese Academy of Sciences, Beijing, 2007), p. 106.
32. H. Lu *et al*., Phytoliths as quantitative indicators for the reconstruction of past environmental conditions in China I: Phytolith-based transfer functions. *Quat. Sci. Rev.* **25**, 945–959 (2006).
33. Y. F. Yue *et al*., A continuous record of vegetation and climate change over the past 50,000 years in the Fujian Province of eastern subtropical China. *Palaeogeogr. Palaeoclimatol. Palaeoecol.* **365**, 115–123 (2012).
34. X. Zhang, Z. Zheng, K. Y. Huang, X. Q. Yang, L. P. Tian, Sensitivity of altitudinal vegetation in southwest China to changes in the Indian summer monsoon during the past 68000 years. *Quat. Sci. Rev.* **239**, 1–16 (2020).
35. H. Y. Lu, K. B. Liu, Morphological variations of lobate phytoliths from grasses in China and the south-eastern United States. *Divers. Distrib.* **9**, 73–87 (2003).
36. Z. Rao *et al*., Relationship between climatic conditions and the relative abundance of modern C_3 and C_4 plants in three regions around the North Pacific. *Chin. Sci. Bull.* **55**, 1931–1936 (2010).
37. S. Yang, Z. Ding, X. Wang, Z. Tang, Z. Gu, Negative $\delta^{18}O$-$\delta^{13}C$ relationship of pedogenic carbonate from northern China indicates a strong response of C_3/C_4 biomass to the seasonality of Asian monsoon precipitation. *Palaeogeogr. Palaeoclimatol. Palaeoecol.* **317**, 32–40 (2012).
38. D. W. Lea, D. K. Pak, H. J. Spero, Climate impact of late quaternary equatorial pacific sea surface temperature variations. *Science* **289**, 1719–1724 (2000).
39. G. Leduc *et al*., Moisture transport across Central America as a positive feedback on abrupt climatic changes. *Nature* **445**, 908–911 (2007).
40. Z. Liu, T. D. Herbert, High-latitude influence on the eastern equatorial Pacific climate in the early Pleistocene epoch. *Nature* **427**, 720–723 (2004).
41. D. W. Lea *et al*., Paleoclimate history of Galapagos surface waters over the last 135,000 yr. *Quat. Sci. Rev.* **25**, 1152–1167 (2006).
42. M. Kienast *et al*., Eastern Pacific cooling and Atlantic overturning circulation during the last deglaciation. *Nature* **443**, 846–849 (2006).
43. D. D. Rousseau, G. Kukla, J. McManus, What is what in the ice and the ocean? *Quat. Sci. Rev.* **25**, 2025–2030 (2006).
44. T. M. Dokken, K. H. Nisancioglu, C. Li, D. S. Battisti, C. Kissel, Dansgaard-Oeschger cycles: Interactions between ocean and sea ice intrinsic to the Nordic seas. *Paleoceanography* **28**, 491–502 (2013).
45. B. M. Vinther *et al*., A synchronized dating of three Greenland ice cores throughout the Holocene. *J. Geophys. Res.-Atmos.* **111**, D13102 (2006).
46. S. O. Rasmussen *et al*., A new Greenland ice core chronology for the last glacial termination. *J. Geophys. Res.-Atmos.* **111**, D06102 (2006).
47. K. K. Andersen *et al*., The Greenland ice core chronology 2005, 15-42 ka. Part 1: Constructing the time scale. *Quat. Sci. Rev.* **25**, 3246–3257 (2006).
48. A. Svensson *et al*., A 60 000 year Greenland stratigraphic ice core chronology. *Clim. Past* **4**, 47–57 (2008).
49. M. Siddall *et al*., Sea-level fluctuations during the last glacial cycle. *Nature* **423**, 853–858 (2003).
50. Y. Dandan, Z. Ren, Z. Yuechao, L. Wan, X. Guo, Correlation between the subtropical high abnormal longitudinal position and the east Asian summer monsoon system. *Daqi Kexue Xuebao* **37**, 304–312 (2014).
51. J. Ma, J. P. Li, The principal modes of variability of the boreal winter Hadley cell. *Geophys. Res. Lett.* **35** (L01808), 1–5 (2008).
52. J. Feng, J. Li, F. Xie, Long-term variation of the principal mode of boreal spring Hadley circulation linked to SST over the Indo-Pacific warm pool. *J. Clim.* **26**, 532–544 (2013).
53. J. Piao, W. Chen, L. Wang, F. S. R. Pausata, Q. Zhang, Northward extension of the east Asian summer monsoon during the mid-Holocene. *Glob. Planet. Change* **184**, 1–9 (2020).
54. G. Leduc, L. Vidal, K. Tachikawa, E. Bard, ITCZ rather than ENSO signature for abrupt climate changes across the tropical Pacific? *Quat. Res.* **72**, 123–131 (2009).
55. G. Yancheva *et al*., Influence of the intertropical convergence zone on the east Asian monsoon. *Nature* **445**, 74–77 (2007).
56. D. McGee, A. Donohoe, J. Marshall, D. Ferreira, Changes in ITCZ location and cross-equatorial heat transport at the last glacial maximum, Heinrich stadial 1, and the mid-Holocene. *Earth Planet. Sci. Lett.* **390**, 69–79 (2014).
57. M. Sheng *et al*., A 20,000-year high-resolution pollen record from Huguangyan Maar Lake in tropical-subtropical South China. *Palaeogeogr. Palaeoclimatol. Palaeoecol.* **472**, 83–92 (2017).
58. S. Yang *et al*., Warming-induced northwestward migration of the east Asian monsoon rain belt from the last glacial maximum to the mid-Holocene. *Proc. Natl. Acad. Sci. U.S.A.* **112**, 13178–13183 (2015).
59. A. Fuhrmann *et al*., Variations in organic matter composition in sediments from lake Huguang Maar (Huguangyan), South China during the last 68 ka: Implications for environmental and climatic change. *Org. Geochem.* **34**, 1497–1515 (2003).
60. S. Wang, H. Lu, J. Liu, Timing of the last deglacial warming in low and middle latitudes of China: Compared with bipolar ice core. *Quat. Sci.* **26**, 283–292 (2006).
61. P. C. Twiss, E. Suess, R. M. Smith, Division S-5-soil genesis, morphology, and classification (morphological classification of grasses phytolith). *Soil Sci. Soc. Am. Proc.* **33**, 109–115 (1969).
62. R. Kondo, C. Childs, I. Atkinson, *Opal Phytoliths of NewZealand* (Manaaki Whenua Press, Canterbury, 1994), p. 85.
63. Y. Wang, H. Lu, *Phytolith Study and its Application* (China Ocean Publishing, Beijing, 1993), p. 228.
64. Institute of Botany and South China Institute of Botany, *Academic Sinica, Angiosperm Pollen Flora of Tropic and Subtropic China* (Science Press, Beijing, 1982), p. 453.
65. F. X. Wang, N. F. Chien, Y. L. Zhang, H. Q. Yang, *Pollen Flora of China* (Science Press, Beijing, ed. 2, 1995), p. 461.
66. S. Juggins, "C2 User Guide: Software for Ecological and Palaeoecological Data Analysis and Visualisation: User Guide Version 1.5" (University of Newcastle, Newcastle upon Tyne, UK, 2003), p. 73.
67. P. J. Reimer *et al*., Intcal13 and marine13 radiocarbon age calibration curves 0-50,000 years cal BP. *Radiocarbon* **55**, 1869–1887 (2013).